Photophysics and Redox Properties of Rylene Imide and Diimide Dyes Alkylated Ortho to the Imide Groups

Joseph E. Bullock, Michael T. Vagnini, Charusheela Ramanan, Dick T. Co, Thea M. Wilson, Jay W. Dicke, Tobin J. Marks,* and Michael R. Wasielewski*

Department of Chemistry and Argonne−Northwestern Solar Energy Research (ANSER) Center, Northwestern University, Evanston, Illinois 60208-3113

Received: September 8, 2009; Revised Manuscript Received: December 21, 2009

Ruthenium-catalyzed C−H bond activation was used to directly attach phenethyl groups derived from styrene to positions ortho to the imide groups in a variety of rylene imides and diimides including naphthalene-1,8-dicarboximide (NMI), naphthalene-1,4:5,8-bis(dicarboximide) (NI), perylene-3,4-dicarboximide (PMI), perylene-3,4:9,10-bis(dicarboximide) (PDI), and terrylene-3,4:11,12-bis(dicarboximide) (TDI). The monoimides were dialkylated, while the diimides were tetraalkylated, with the exception of NI, which could only be dialkylated due to steric hindrance. The absorption, fluorescence, transient absorption spectra, and lowest excited singlet state lifetimes of these chromophores, with the exception of NI, are nearly identical to those of their unsubstituted parent chromophores. The reduction potentials of the dialkylated chromophores are ∼100 mV more negative and oxidation potentials are ∼40 mV less positive than those of the parent compounds, while the corresponding potentials of the tetraalkylated compounds are ∼200 mV more negative and ∼100 mV less positive than those of their parent compounds, respectively. Continuous wave electron paramagnetic resonance (EPR) and electron nuclear double resonance (ENDOR) data on the radical anion of PDI reveals spin density on the perylene-core protons as well as on the β-protons of the phenethyl groups. The phenethyl groups enhance the otherwise poor solubility of the bis(dicarboximide) chromophores and only weakly perturb the photophysical and redox properties of the parent molecules, rendering these derivatives and related molecules of significant interest to solar energy conversion.

Introduction

For decades, rylene imide dyes have been intensively studied as useful light absorbers,[1−15] fluorescent tags,[6,16,17] and electron donors/acceptors.[2,4,18−30] The naphthalene derivatives, naphthalene-1,8-dicarboximides (NMI) and naphthalene-1,4:5,8-bis(dicarboximides) (NI), have been used in artificial photosynthetic systems,[2,24,31,32] while the higher homologues, perylene-3,4-dicarboximides (PMIs),[3,6,8,17] perylene-3,4:9,10-bis(dicarboximides) (PDIs),[3,5,6] and terrylene-3,4:11,12-bis(dicarboximides) (TDIs),[3,8,9,33,34] have been extensively researched not only in artificial photosynthetic systems[24,35] but also in light-harvesting systems[36−38] and in solid-state devices such as organic field-effect transistors[21,28] and photovoltaics.[18,20,22,23,25,29,30,39,40] In all these systems, chemical functionalization through the imide group has been shown to proceed efficiently starting from either the dicarboxylic acid[15] or the cyclic anhydride.[11,17,18,34] Molecular orbital calculations on these systems show that they all exhibit a nodal plane in both their HOMO and LUMO that bisects the molecules through the imide nitrogen(s), which decouples the imide substituent from the π electronic structure of the rylene imide or diimide chromophore.[3,41−43] Thus, a diverse array of alkyl and aryl imide derivatives of these dyes have been prepared in which the *N*-alkyl or *N*-aryl groups have negligible impact on the optical and electrochemical properties of the chromophores. The covalent synthesis of multichromophoric arrays demands exploitation of the imide functionality in such a way that each chromophore retains its inherent properties.

The insolubility of these systems, especially the larger perylene and terrylene derivatives, necessitates the use of bulky solubilizing groups, which are commonly attached to the "bay regions" of the aromatic core via heteroatoms. In addition to imparting solubility, these substitutions affect the optical and electronic properties of the dyes. Würthner and co-workers have reported di-, tri-, and tetra-substituted NI-based chromophores with optical transitions that span 400−650 nm.[7,11,13,14,42] They have also demonstrated numerous substitutions in the bay region (1-, 6-, 7-, and 12-positions) of PDI derivatives with various phenoxy groups.[39] Rybtchinski and co-workers have described the synthesis of water-soluble PDI derivatives, which also possess alkyne connections.[40,41,44,45] Separately, they have reported PDI derivatives which possess transition metals in the bay region. Furthermore, Huang et al. demonstrated several examples of thiophenes attached to the bay region positions of PDI,[46] and Müllen and co-workers have pioneered many of the synthetic strategies for functionalizing the bay positions of TDI with phenoxy, cyclic amine, and even water-soluble moieties.[3,8,9] Some of our own studies include amino-substituted PDIs with desirable electron-donating properties,[47,48] and cyanated NIs and PDIs,[21,28] which have some of the highest electron mobilities observed for organic semiconductors. Formation of various unsaturated C−C substituents on the aromatic core has been demonstrated with NI, PMI, and PDI using palladium-catalyzed cross-coupling reactions.[12,45,49−51] The synthetic strategies for functionalizing rylene imides are numerous and have enabled researchers to span the optical absorption range from the blue to the near-infrared region, as well as span redox potentials from −1.4 to 1.6 V vs SCE. All the aforementioned substitutions require bromination or chlorination of the aromatic core, which is typically performed

* To whom correspondence should be addressed. E-mail: m-wasielewski@northwestern.edu.

10.1021/jp908679c
Published on Web 01/14/2010

under highly acidic conditions.[14,15,21,31,44,47] Halogenation of PMI, PDI, and TDI typically takes place in the bay region, and the steric consequences of bay substitution disrupt the planarity of the aromatic core, adversely affecting their electronic structures.[27,52] To minimize this effect, synthetic strategies must avoid substitution in the bay region and create saturated C−C bonds in lieu of heteroatomic substitution. Until very recently,[53] an efficient method for functionalizing rylene imides with saturated C−C bonds, and chemically accessing the position ortho to the imide, has not been available due to the electron-withdrawing effect of the imides. Such substitutions would be beneficial for solubility while maintaining the optical properties of the parent chromophore.

In the early 1990s, Murai et al. pioneered the use of ruthenium catalysts for highly efficient aromatic C−H bond activated coupling to olefins.[54−61] They discovered that $Ru(H_2)CO(PPh_3)_3$ selectively coordinates with aromatic ketones to generate new saturated C−C bonds α to the carbonyl and observed the greatest reactivity with more electron-deficient substrates. The efficiency and versatility of these catalytic reactions prompted their use in polymer chemistry[62−64] as well as in forming unsaturated C−C bonds.[65] Recently, Osuka et al. reported the first example of using $Ru(H_2)CO(PPh_3)_3$ to selectively alkylate the ortho positions of PDI.[53] We have now extended this work to include a broad range of rylene imides and diimides of importance to both organic electronics and solar energy conversion. Electrochemistry, steady-state, transient optical, electron paramagnetic resonance (EPR), and electron nuclear double resonance (ENDOR)spectroscopy have been used to fully determine the effects of this new substitution pattern on the electronic, photophysical, and redox properties of these new chromophores.

Synthesis. Ruthenium-catalyzed C−H bond activation reactions are generally performed in toluene at elevated temperatures.[66] However, since we were attempting 4-fold coupling reactions, we used higher boiling mesitylene to decrease reaction times.[53] All parent dyes (**1**,[7] **3**,[7] **5**,[17] **7**,[19] and **9**[9]) were synthesized according to published procedures. Styrene and $Ru(H_2)CO(PPh_3)_3$ were purchased from Aldrich and used without further purification. All glassware was flame-dried and kept stringently free from O_2. All synthesized compounds were analyzed at Northwestern University (IMSERC) using a Varian 500 MHz NMR, and high-resolution mass spectrometry was performed on a Bruker MALDI-TOF instrument with polystyrene as an internal standard.

Electrochemistry. Electrochemical measurements were performed using a CH Instruments Model 622 electrochemical workstation. Measurements for **4**, **6**, **8**, and **10** were performed in dichloromethane containing 0.1 M tetrabutylammonium hexafluorophosphate ($TBAPF_6$) electrolyte. Measurements for compound **2** were performed in benzonitrile with the same electrolyte. A 1.0 mm diameter platinum disk electrode, platinum wire electrode, and Ag/AgO^+ reference electrode were employed. The ferrocene/ferrocenium redox couple (Fc/Fc^+, 0.46 V vs SCE)[67] was used as an internal standard. $TBAPF_6$ was recrystallized twice from ethyl acetate prior to use.

Optical Spectroscopy. Steady-state electronic absorption spectra were recorded on a Shimadzu 1601 UV/vis spectrometer with a 2 mm quartz cuvette. Fluorescence measurements were performed using a PTI Quanta-Master 1 single-photon-counting spectrofluorimeter in a right angle configuration with a 1 cm quartz cuvette.

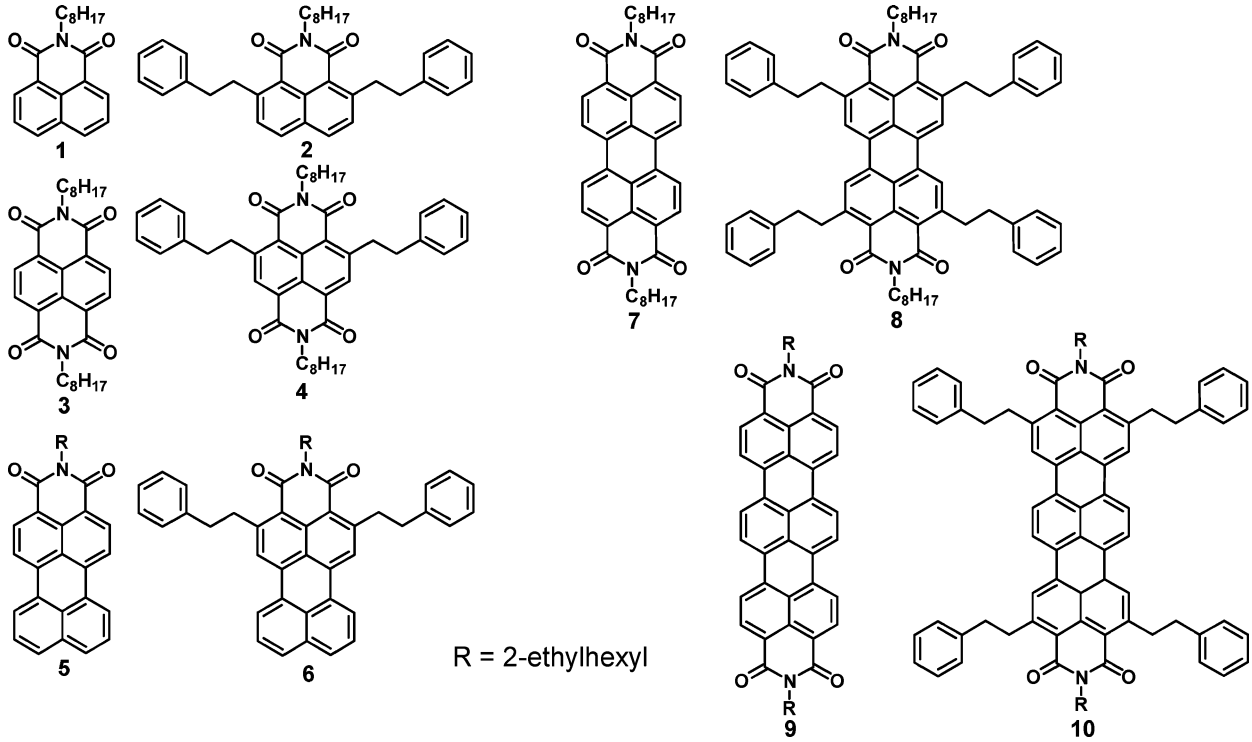

Experimental Section

Solvents. Mesitylene was purchased from Aldrich, distilled over CaH_2, and stored over molecular sieves. Toluene (Aldrich) and nonstabilized HPLC grade dichloromethane (DCM) (Fisher) were dried using a Glass Contour solvent system.

Femtosecond transient absorption measurements were made using a 2 kHz Ti:sapphire laser system as detailed previously,[68] with the exception that the original oscillator has been replaced with a Spectra-Physics Tsunami. The wavelengths used to excite the samples were 390 nm (**1**−**4**), 416 nm (**5**−**8**), and 650 nm (**9**−**10**). The instrument response function for the pump−probe experiments is 150 fs. The transient spectra were obtained using

SCHEME 1: NI Reaction Intermediate Illustrating the Steric Hindrance Impeding Incorporation of More than Two Substituents

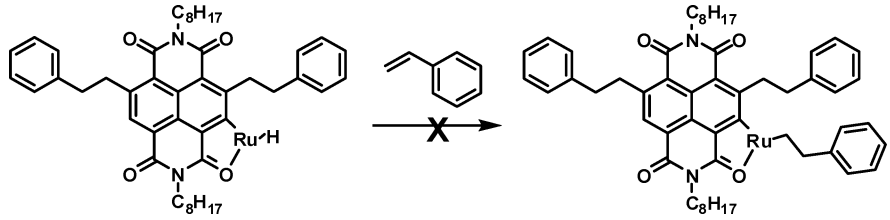

SCHEME 2: Alkylation Results for Compound 7

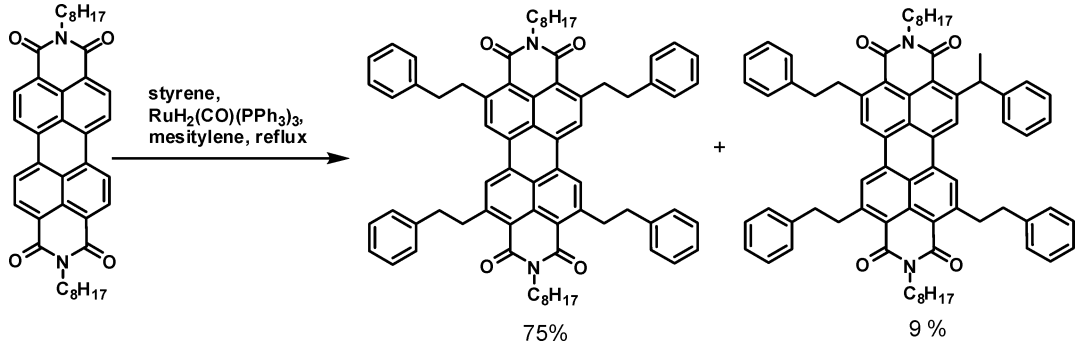

5 s of averaging at a given delay time. Glass cuvettes with a 2 mm path length were used and the samples were dissolved in dry solvent and irradiated with 1.0 μJ pulses at the excitation wavelength.

Time resolved fluorescence measurements were performed at the Center for Nanoscale Materials at Argonne National Laboratory using a frequency-doubled, mode-locked Ti:sapphire laser system (Coherent Mira-900) with a 76.5 MHz repetition rate to generate 416 nm pulses to excite **6** and **8**. An optical parametric oscillator (Coherent Mira-OPO) was used to generate 550 nm pulses to excite **9** and **10**. Short- and long-pass filters were used to remove residual pump radiation. Glass cuvettes with a 1 cm path length were used, and the samples were dissolved in dry solvent and irradiated with 100−300 μW of pump light. The fluorescence emitted at right angles was detected with a fiber-coupled avalanche photodiode (PDM from Micro Photon Devices). The time-correlated single-photon-counting module was a PicoHarp 300 from PicoQuant. The instrument response function using 416 nm pulses was 270 ps, while that using the 550 nm pulses was 35 ps. Analyses of the kinetic data for both the transient absorption and fluorescence lifetime experiments were performed by using a Levenberg−Marquardt nonlinear least-squares fit to a general sum-of-exponentials function convoluted with a Gaussian instrument response function.

EPR and ENDOR Spectroscopy. Continuous wave EPR and ENDOR spectra were acquired with a Bruker Elexsys E580 spectrometer, fitted with the DICE ENDOR accessory, EN801 resonator, and an ENI A-500 rf power amplifier. Rf powers ranged from 240 to 400 W across the 7 MHz scanned range, and microwave power was 2−6 mW. The sample temperature of 290 K was controlled by a liquid nitrogen flow system. All samples and solvents were handled in a nitrogen atmosphere glovebox (MBraun Unilab). Samples were prepared in DCM with 2% triethylamine (TEA) (w/w) and loaded into 1.4 mm I.D. quartz tubes which were sealed with a 0.5−1.0 cm plug of vacuum grease and wrapped tightly with Parafilm. TEA was dried with CaH_2 and filtered through dry silica gel prior to use and storage in the glovebox. Photochemical reduction to form monoanions was accomplished by exciting the sample with an Ar^+ laser (514.5 nm, 40 mW) beam elongated in one dimension with a cylindrical lens. In all cases the photochemical reductions using TEA formed solely monoanions of the PDI oligomers as monitored by UV−vis. UV−vis spectra acquired through the quartz tube match the spectra of PDI radical anions generated electrochemically. A spline fit baseline correction was applied to the ENDOR spectra following integration.

Density Functional Theory (DFT) Calculations. The structure of a model PDI radical anion with ethyl substituents at the 2, 5, 8, and 11 positions, as well as at the imide positions, was first optimized using unrestricted DFT with Q-Chem 3.1[69] at the B3LYP/6-31G* level. A single-point unrestricted DFT calculation at this optimized geometry was performed to calculate the isotropic hyperfine coupling constants (hfcc's) using a B3LYP functional with the expanded double-ζ EPR-II basis set[70] and Gaussian 98W.[71]

Results and Discussion

Synthesis. Reacting naphthalene monoimide **1** with styrene in the presence of $Ru(H_2)CO(PPh_3)_3$ produces the dialkylated product **2** in 49% yield. Contrary to our expectations, however, reacting the corresponding naphthalene diimide **3** under the same conditions leads to a 1:1 isomeric mixture of 2,6- and 2,7-disubstituted products in 48% yield. We surmise that steric hindrance inhibits 4-fold substitution, as ruthenium-catalyzed C−H bond activation reactions are significantly influenced by steric factors.[61,65] Even with extended reaction times,[72] the Ru catalyst cannot effectively bind the carbonyl group to activate the proximal C−H bond, and hence realize styrene coupling in the presence of an adjacent phenethyl group (Scheme 1). This apparently prohibits styrene coordination to the ruthenium, a prerequisite for C−C bond formation. The 2,7-disubstituted isomer, **4**, was isolated by HPLC to determine its photophysical and redox properties. The dialkylated perylene monoimide **6** was readily prepared from **5** in 72% yield, while the corresponding tetraalkylated PDI **8** was formed in 75% yield from **7** in agreement with the initial report of Osuka et al.[53] In preparing **8**, we also isolated a small percentage of an isomeric byproduct containing a single 1-phenylethyl group (Scheme 2),[65] which could be separated from the target product using preparative

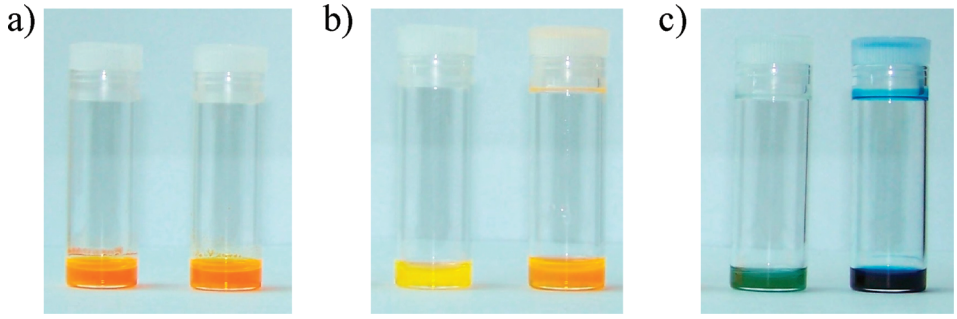

Figure 1. Photographs of saturated toluene solutions of (a) **PMI**, (b) **PDI**, and (c) **TDI**. In each photo, the left vial contains bare chromophore (**5**, **7**, and **9**) while the right vial contains alkylated chromophore (**6**, **8**, and **10**).

TABLE 1: Solubilities of Alkylated vs Non-alkylated Rylene Chromophores

chromophore	solubility[a] (mg/mL)
5	2
6	6
7	<1
8	2
9	<1
10	3

[a] Measured in toluene.

TLC. Reducing the amount of catalyst in the reaction did not lower the yield of byproduct, which has been observed previously in C−H activation reactions of aryl ketones.[65] The higher homologue, terrylenediimide **9**, was tetraalkylated to give **10** in 81% yield; however, no isomerization of the phenethyl groups was observed in this reaction. The larger ring systems (**5**, **7**, and **9**) all give much higher yields of substitution, most likely a result of reduced steric hindrance.

The phenethyl groups have a significant effect on the solubility of the larger ring systems (Figure 1). While compound **5** has significant solubility in toluene due to the branched alkyl chain at the imide nitrogen atom, **6** has 3 times the solubility with only two substituents (Table 1). A saturated solution of **7** in toluene is only weakly colored, yet exhibits a strong yellow fluorescence under ambient light; in contrast, **8** dissolves to give a significantly darker solution (Figure 1). Compound **9** possesses two branched imide chains, but is similar to **7** in terms of solubility. However, the addition of four phenethyl groups significant increases its solubility. With its high extinction coefficient (80 000 M^{-1} cm^{-1}), saturated solutions of **10** in toluene are virtually opaque.

Redox Potentials. Substitution of the phenethyl groups ortho to the imide nitrogen atom renders these chromophores somewhat more difficult to reduce, but easier to oxidize (Table 2). The reduction potentials of the disubstituted chromophores (**2**, **4**, **6**) are approximately 130 mV more negative than those of their parent compounds. Correspondingly, the oxidation potential of the disubstituted **6** is 40 mV less positive than that of **6**. Tetrasubstituted **8** and **10** have reduction potentials that are more negative by ~200 mV than their unsubstituted analogues. These shifts in redox potentials reasonably arise from the electron-donating nature of the phenethyl groups. The oxidation and reduction potentials of all alkylated molecules shift in the same direction by nearly the same amount, such that the corresponding HOMO−LUMO energy gap remains essentially the same, as is reflected in their electronic absorption and emission spectra described below.

Electronic Absorption and Emission Spectra. The ground-state electronic absorption spectra for **2**, **4**, **6**, **8**, and **10** are shown in Figure 2a. The intensity of the $S_0 \rightarrow S_1$ transition increases with the size of the aromatic core, while the energy decreases. The fluorescence spectrum of each chromophore is shown in Figure 2b and summarized in Table 3 along with those of compounds **1**, **3**, **5**, **7**, and **9**. We see a similar trend in the emission maxima, which move to longer wavelengths as the size of the aromatic core increases. The electronic absorption and fluorescence properties of all the alkylated chromophores are very similar to those of the parent compounds. No observable trend is apparent for the slight shifts in λ_{max}; however, with the exception of **2**, all alkylated compounds have slightly lower extinction coefficients than their parent compounds. The fluorescence emission maxima of the alkylated compounds (Table 3) are similar to those of the parent compounds: **1**,[32] **3**,[73] **5**,[8] **7**,[1] and **9**.[8] However, the phenethyl groups significantly reduce the fluorescence quantum yields of only the naphthalene derivatives **2** and **4**, while the yields for the higher rylenes are unaffected. A possible mechanism for the reduced fluorescence quantum yields of **2** and **4** relative to those of **1** and **3**, respectively, will be discussed below.

TABLE 2: Redox Potentials (V vs SCE) of the Alkylated and Unsubstituted Chromophores

chromophore	$E^{+}_{1/2}$	$E^{-}_{1/2}$	$E^{2-}_{1/2}$
1	−	−1.40[a]	−
2	−	−1.53[b]	−
3	−	−0.48[a]	−0.99[a]
4	−	−0.61,	−1.15
5	1.41	−1.00[c]	−1.49[c]
6	1.37	−1.13	−1.43
7	1.67	−0.50[c]	−0.73[c]
8	1.63	−0.75	−0.93
9	1.12	−0.63[c]	−
10	1.00	−0.83	−

[a] Ref 5. [b] Obtained in benzonitrile with 0.1 M $TBAPF_6$. [c] Ref 3.

The absorption spectrum of the radical anion of **8** was obtained by photoreduction in the presence of triethylamine in CH_2Cl_2. As **8** is reduced, absorption bands at 691 (shoulder 645 nm), 774 (shoulder 796 nm), 824, and 910 nm appear and the vibronic progression of the neutral species in the visible region decreases in intensity (Figure S1, Supporting Information). The absorption spectrum of $\mathbf{8}^{\bullet-}$ is similar to that of other PDI radical anion derivatives.[5]

Transient Absorption and Emission Spectroscopy. The transient absorption spectra of naphthalene monoimide **2** are shown in Figure 3. The $S_1 \rightarrow S_n$ absorption is characterized by a single broad band near 575 nm, which decays monoexponentially with a time constant $\tau_D = 34$ ps. This is similar to the time constant obtained for other NMI derivatives[4] and is attributed to rapid intersystem crossing leading to the triplet state of **2**. The transient absorption spectra and monoexponential

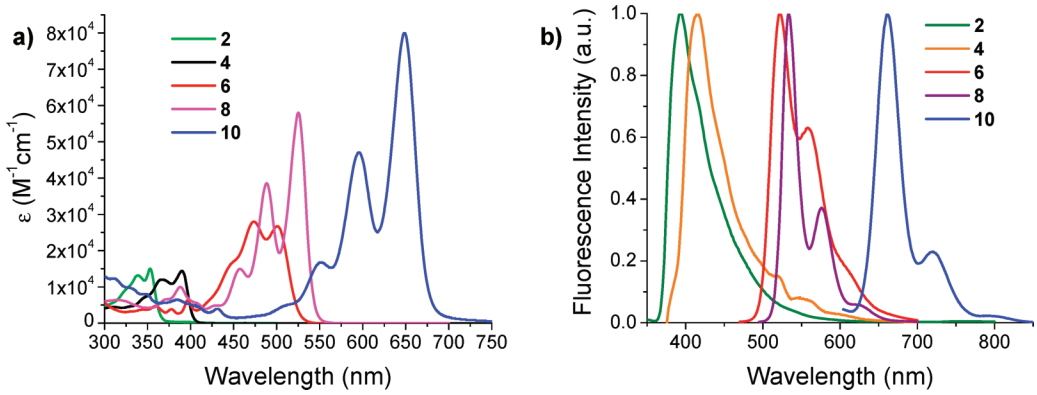

Figure 2. (a) UV−vis absorption and (b) fluorescence spectra of rylene chromophores in toluene.

TABLE 3: Electronic Absorption (λ_{max}) and Emission Maxima (λ_{em}), S_1 Energies, Fluorescence Quantum Yields (ϕ_F) and Fluorescence Lifetimes (τ_{S1}) in Toluene

chromophore	λ_{max} (nm) (ε ($M^{-1}cm^{-1}$))	λ_{em} (nm)	$E(S_1)^c$ (eV)	ϕ_F	τ_{S1} (ns)
1	350 (10647)[a]	386[a]	3.38	0.25[d]	<0.005[i]
2	353 (15000)	394	3.34	0.08	0.034 ± 0.001
3	382 (14500)[a]	407[a]	3.15	0.0018[e]	<0.002[i]
4	390 (14000)	415	3.09	0.0005	0.0016 ± 0.0009
5	505 (29970)[a]	539[a]	2.38	0.98[f]	3.5 ± 0.1[j]
6	501 (27000)	521	2.43	0.98	6.8 ± 0.1
7	526 (80000)[a]	535[a]	2.34	0.99[g]	4.5 ± 0.1
8	525 (58000)	533	2.35	0.99	5.1 ± 0.1
9	650 (93000)[b]	673[b]	1.88	0.95[h]	3.5 ± 0.1
10	649 (80000)	661	1.90	0.95	3.4 ± 0.1

[a] Reference 5. [b] Reference 34. [c] Determined from the average energy of the absorption and emission maxima. [d] Reference 32. [e] Reference 73. [f] Reference 8. [g] Reference 1. [h] Reference 8. [i] Reference 4. [j] Reference 33.

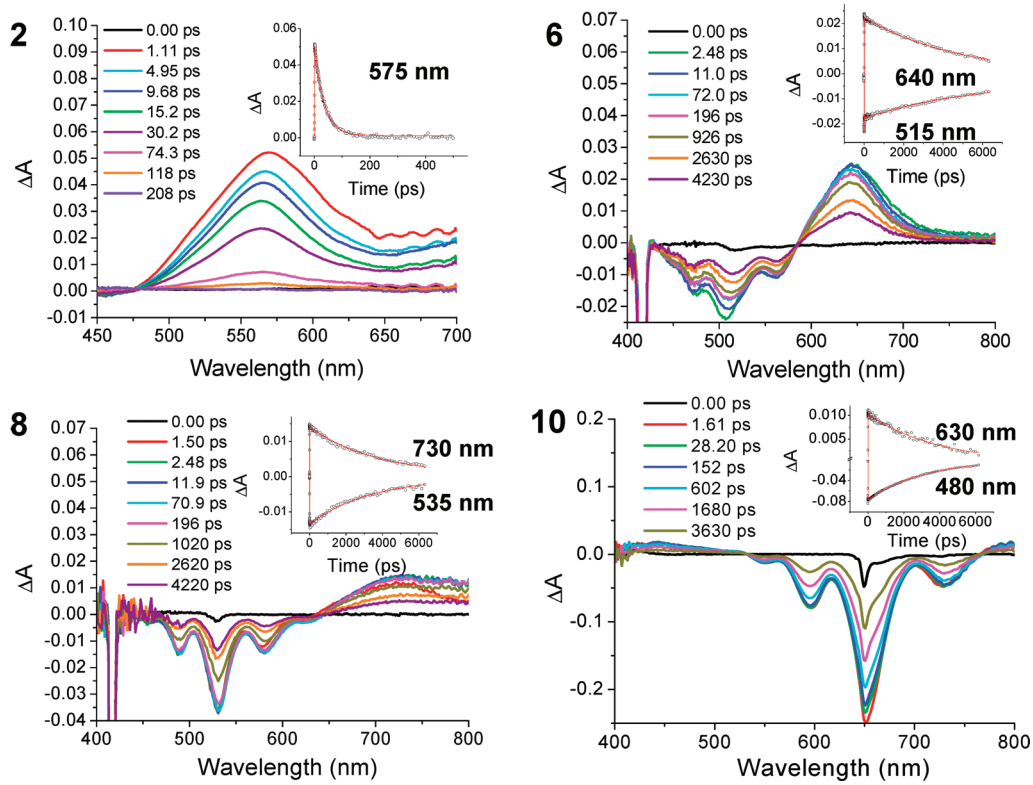

Figure 3. Transient absorption spectra of compounds **2, 6, 8,** and **10** in toluene. Insets: transient absorption kinetics at the indicated wavelengths. The sharp negative features observed in the spectra of **6**, **8**, and **10** at 416, 416, and 650 nm, respectively, are due to scatter from the excitation laser pulse.

S_1 lifetimes of the perylene derivatives **6** and **8** are similar to those reported by us earlier for other PMI and PDI derivatives,[4,74] and are illustrative of the minimal perturbation that the (two) four alkyl substituents have on the electronic structures of these molecules (Table 3). The transient absorption spectrum of a terrylenediimide has not been reported previously and is shown

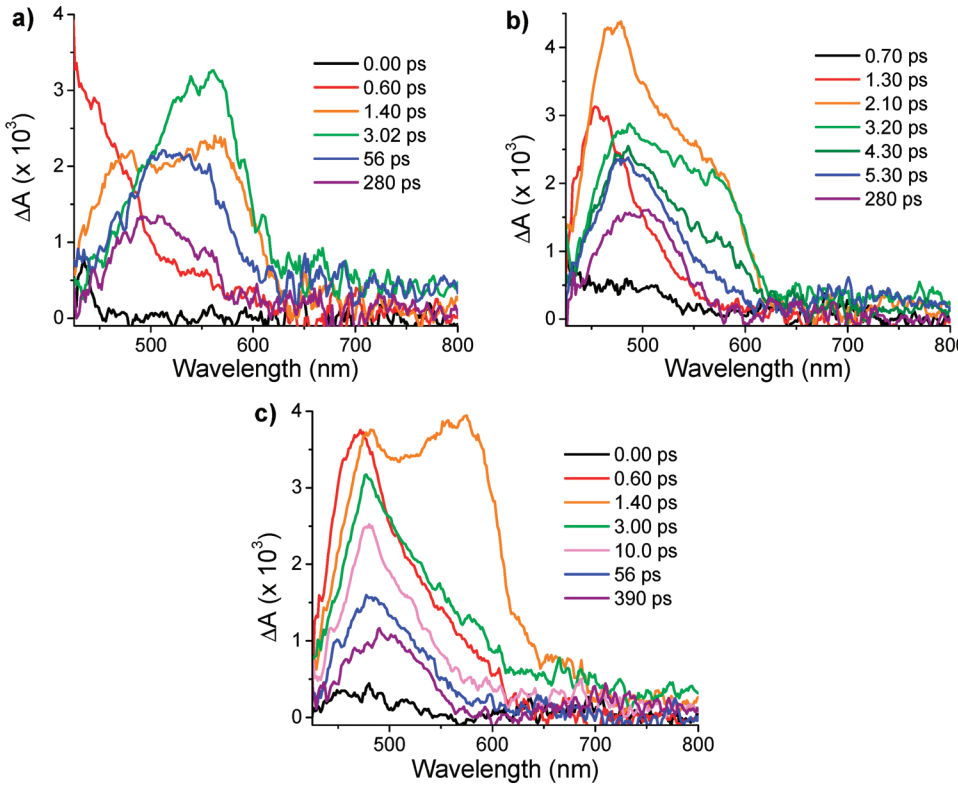

Figure 4. Transient absorption spectra of **4** in (a) toluene, (b) MTHF, and (c) PrCN.

for **10** in Figure 3. The bleaching of the ground-state absorption bands is accompanied by a strong stimulated emission feature at 725 nm, as well as weak positive absorption changes at 400−540 nm and 765−800 nm. All of these transient spectral changes decrease with a monoexponential decay time of τ_{S1} = 3.4 ns, which is very similar to that observed previously for **9** using time-resolved fluorescence measurements.[33]

Time-resolved fluorescence experiments were also conducted in order to more accurately determine the singlet excited-state lifetimes for **6**, **8**, **9**, and **10** (Table 3), given that the maximum pump−probe delay time available using our femtosecond transient absorption apparatus is about 6 ns. As expected, there is no significant solvent dependence (Table S1, Supporting Information). The fluorescence lifetimes of **8** and **10** are very similar to those of their respective unsubstituted analogues **7** and **9**, while that of **6** is only about twice as long as that of **5**. Comparing the fluorescence lifetimes of the perylenediimides **7** and **8** with those of the terrylenediimides **9** and **10**, since the fluorescence quantum yields of the terrylenediimides are slightly smaller than those of the perylenediimides, the somewhat shorter S_1 lifetimes of the terrylenediimides result largely from a small increase in their nonradiative decay rates due to their smaller S_0-S_1 energy gap.

In contrast to the other phenethyl-substituted rylenes, photoexcitation of the NI group within **4** results in a complex series of solvent-dependent transient absorption spectra and kinetics. Experiments were performed in a series of solvents ranging from low to high polarity, toluene, 2-methyltetrahydrofuran (MTHF), and butyronitrile (PrCN) (Figure 4). Photoexcited naphthalene diimide derivatives have been shown to oxidize phenyl rings covalently bonded to them through their imide nitrogen atoms due to their high excited state energies (E_{S1} = 3.2 eV).[75] Chaignon et al.[31] have demonstrated that electron transfer reaction rates from donors attached to the 2-position of NI are about 1000-fold faster than the rates from donors attached through the imide nitrogen atoms, so that it is likely that photoinduced electron transfer occurs very rapidly from one of the appended phenyl groups to NI in **4**. Following photoexcitation of **4** in all three solvents, a broad feature at 450−500 nm forms within the 150 fs instrument response function, which is assigned to ^{1}*NI. This is followed by rapid, solvent-independent formation (<1 ps) and decay (<2 ps) of a distinct absorption band at 580 nm leading to a longer-lived feature with an absorption maximum near 480 nm, which is characteristic of $NI^{\bullet-}$ formation.[5] The absorption band of $NI^{\bullet-}$ decays much more slowly in low polarity toluene relative to higher polarity MTHF and PrCN (Table 4).

TABLE 4: Kinetics of Exciplex Formation (τ_{ER}) and Decay (τ_{ED}) and the Decay of the Ion Pair (τ_{CR}) in Compound 4

solvent	τ_{ER} (ps)	τ_{ED} (ps)	τ_{CR} (ps)
PrCN	<1	1.2 ± 0.5	2.5 ± 0.5
MTHF	<1	1.4 ± 0.6	1.5 ± 0.7
toluene	<1	1.6 ± 0.9	11.5 ±1.0

We hypothesize that following photoexcitation of NI, rapid electron transfer from one phenyl group to ^{1}*NI occurs resulting in a sandwich-like conformation characteristic of exciplex or tight ion pair formation, which absorbs at 580 nm. Rapid relaxation of this exciplex results in full charge separation to form $Ph^{\bullet+}-NI^{\bullet-}$, which produces the transient absorption characteristic of $NI^{\bullet-}$ near 480 nm. The bandwidth of the $NI^{\bullet-}$ absorption narrows in the more polar solvents that better solvate the $Ph^{\bullet+}-NI^{\bullet-}$ ion pair. Charge recombination of $Ph^{\bullet+}-NI^{\bullet-}$ occurs more rapidly in more polar MTHF and PrCN than in toluene as predicted by energy gap law considerations based on Marcus electron transfer theory.[76] To further test this hypothesis, we performed transient absorption experiments on **4** in MTHF at low temperatures to limit the motion of the phenyl groups relative to NI. The transient absorption spectral features at 193 K (Figure 5a) and 143 K (Figure 5b) are similar to those

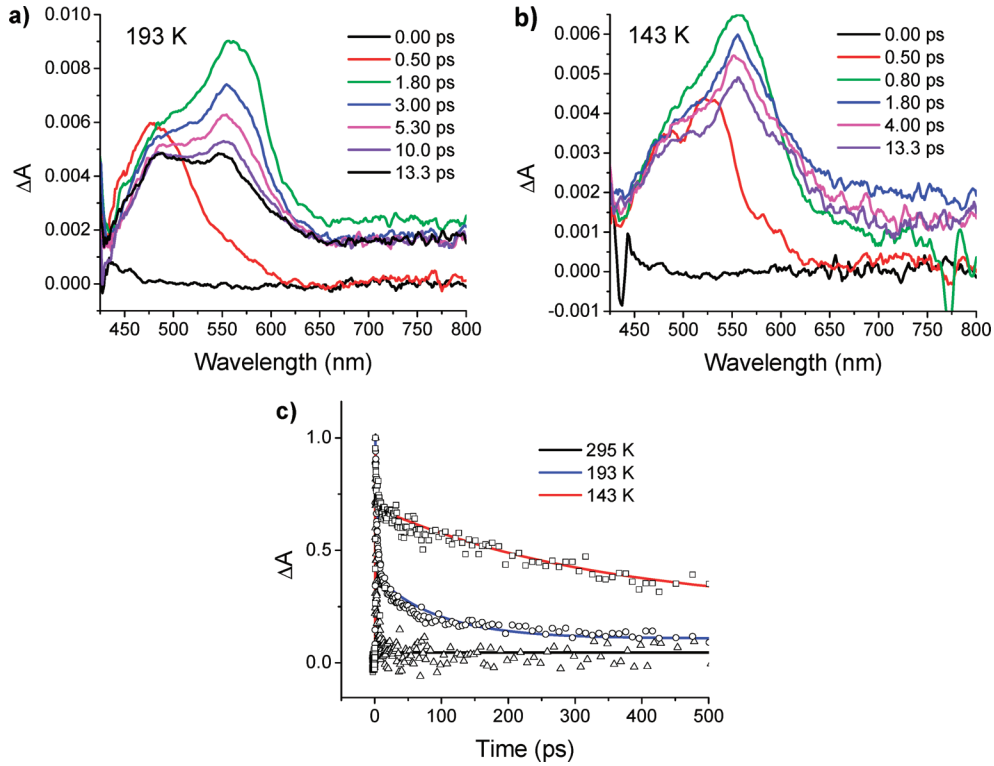

Figure 5. Transient absorption spectra of **4** in MTHF at (a) 193 K and (b) 143 K. (c) Transient kinetics of **4** at 580 nm in MTHF at the indicated temperatures.

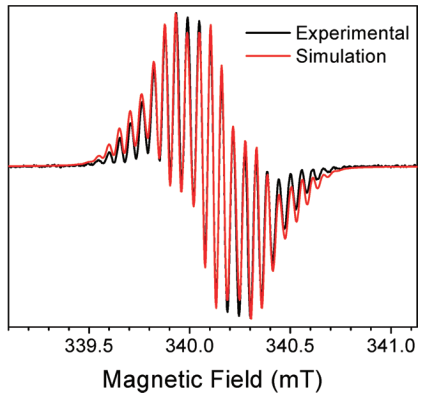

Figure 6. EPR spectra of $\mathbf{8}^{\bullet-}$ in CH_2Cl_2 with ~2% TEA at 290 K. The microwave power was 2 mW with a modulation amplitude of 0.1 G at 25 kHz. The simulation is constrained by ENDOR data for protons, and the nitrogen hfcc is optimized.

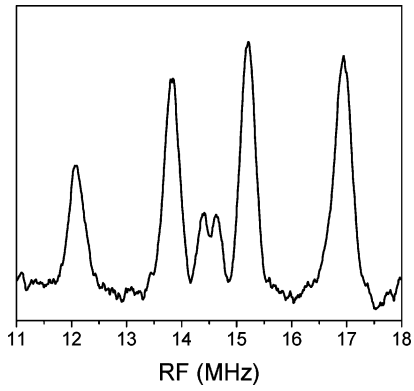

Figure 7. ^{1}H-ENDOR spectra of $\mathbf{8}^{\bullet-}$ in CH_2Cl_2 with ~2% TEA (w/w) at 290 K. Microwave power was 6 mW, and rf power was 240−400 W with a frequency modulation depth of 50 kHz.

observed at 295 K; however, the 580 nm band becomes more pronounced as the temperature decreased. This result suggests that a ground-state charge transfer interaction may fold the phenyl into an exciplex-like conformation with NI prior to excitation as the temperature is lowered. Following photoexcitation of NI at low temperatures, the conformation of the exciplex (tight ion pair) relaxes to the fully solvated ion pair state much more slowly than it does at room temperature, which results in the much longer lifetimes for the 580 nm exciplex absorption band observed at low temperatures (Figure 5c).

EPR and ENDOR Spectroscopy. The EPR spectrum of $\mathbf{8}^{\bullet-}$ (Figure 6) is inhomogeneously broadened due to the large number of hyperfine coupling constants (hfcc's). Isotropic hfcc's were obtained from ENDOR spectroscopy in liquid CH_2Cl_2 at the ENDOR resonance condition $\nu^{\pm}_{ENDOR} = |\nu_n \pm a_H/2|$, where $\nu^{\pm}_{ENDOR}$ are the ENDOR transition frequencies and ν_n is the proton Larmor frequency.[77] The ENDOR spectrum of $\mathbf{8}^{\bullet-}$ obtained at 290 K is presented in Figure 7 and exhibits three line pairs with hfcc's of 4.9, 1.4, and 0.2 MHz. The largest hfcc has been assigned to that of the bay-region protons (positions 1, 6, 7, and 12) on the perylene core and is similar in magnitude to previously reported PDI derivatives.[26,78] The two smaller proton hfcc's are attributed to the β-protons on the phenethyl groups. The 0.2 MHz splitting could also be due to the octyl group attached to the imide nitrogen atom.

These assignments were confirmed using unrestricted DFT to calculate the hfcc's using B3LYP functionals with the expanded double-ζ EPR-II basis set. The computed proton hfcc's were 5.4 (perylene protons 1, 6, 7, 12), 1.6 (β-phenethyl protons), and 0.3 (β-phenethyl and β-octyl protons) MHz and 1.7 MHz for the nitrogens. A simulation of the EPR spectrum of $\mathbf{8}^{\bullet-}$ (Winsim)[79] using the ENDOR results to lock the hfcc values allows determination of the nitrogen hfcc to be 1.4 MHz, which is also in reasonable agreement with the DFT calculation. The EPR and ENDOR spectra reveal that the spin (and charge)

distribution within the radical ion of **8** is very similar to that of PDI, so that one may anticipate that applications of these molecules as electron acceptors would result in similar electron donor−acceptor behavior to that of the unsubstituted molecule except for the alkylated PDI being somewhat more difficult to reduce than the parent molecule.

Conclusions

The catalytic addition of phenethyl groups to rylene imides and diimides yields solublized imide dyes without the need for strongly electron donating heteroatoms or bay-region substituents that may twist the aromatic core and alter the photophysics and redox properties. The versatility of the present alkylation process lends itself to addition of a wide variety of terminal alkenes,[72] providing a broad range of options for tuning rylene solubility and solid-state properties. These new rylene imides and diimides significantly broaden the scope of redox-active chromophores of interest in molecular systems for solar energy conversion.

Acknowledgment. This work was supported by the Chemical Sciences, Geosciences, and Biosciences Division, Office of Basic Energy Sciences, DOE under grants DE-FG02-99ER14999 (M.R.W.) and DE-FG02-08ER46536/A000 (T.J.M.). Use of the Center for Nanoscale Materials was supported by the U.S. Department of Energy, Office of Science, Office of Basic Energy Sciences, under Contract No. DE-AC02-06CH11357. We thank Dr. J. Vura-Weis for assistance with the DFT calculations and Dr. D. Gosztola for assistance with the time-resolved fluorescence measurements.

Supporting Information Available: Synthesis and characterization of **2**, **4**, **6**, **8**, and **10**, time-resolved fluorescence spectra for **6**, **8**, **9**, and **10**, and low-temperature transient absorption studies of **4**. This material is available free of charge via the Internet at http://pubs.acs.org.

References and Notes

(1) Sadrai, M.; Hadel, L.; Sauers, R. R.; Husain, S.; Krogh-Jespersen, K.; Westbrook, J. D.; Bird, G. R. *J. Phys. Chem.* **1992**, *96*, 7988–7996.
(2) Greenfield, S. R.; Svec, W. A.; Gosztola, D.; Wasielewski, M. R. *J. Am. Chem. Soc.* **1996**, *118*, 6767–6777.
(3) Lee, S. K.; Zu, Y.; Herrmann, A.; Geerts, Y.; Muellen, K.; Bard, A. J. *J. Am. Chem. Soc.* **1999**, *121*, 3513–3520.
(4) Hayes, R. T.; Wasielewski, M. R.; Gosztola, D. *J. Am. Chem. Soc.* **2000**, *122*, 5563–5567.
(5) Gosztola, D.; Niemczyk, M. P.; Svec, W.; Lukas, A. S.; Wasielewski, M. R. *J. Phys. Chem. A* **2000**, *104*, 6545–6551.
(6) Sussmeier, F.; Langhals, H. *Eur. J. Org. Chem.* **2001**, 607–610.
(7) Wuerthner, F.; Ahmed, S.; Thalacker, C.; Debaerdemaeker, T. *Chem.−Eur. J.* **2002**, *8*, 4742–4750.
(8) Weil, T.; Reuther, E.; Beer, C.; Muellen, K. *Chem.--Eur. J.* **2004**, *10*, 1398–1414.
(9) Nolde, F.; Qu, J. Q.; Kohl, C.; Pschirer, N. G.; Reuther, E.; Muellen, K. *Chem.−Eur. J.* **2005**, *11*, 3959–3967.
(10) Addicott, C.; Oesterling, I.; Yamamoto, T.; Muellen, K.; Stang, P. J. *J. Org. Chem.* **2005**, *70*, 797–801.
(11) Thalacker, C.; Roeger, C.; Wuerthner, F. *J. Org. Chem.* **2006**, *71*, 8098–8105.
(12) Chopin, S.; Chaignon, F.; Blart, E.; Odobel, F. *J. Mater. Chem.* **2007**, *17*, 4139–4146.
(13) Roeger, C.; Ahmed, S.; Wuerthner, F. *Synthesis* **2007**, 1872–1876.
(14) Roeger, C.; Wuerthner, F. *J. Org. Chem.* **2007**, *72*, 8070–8075.
(15) Kishore, R. S. K.; Ravikumar, V.; Bernardinelli, G.; Sakai, N.; Matile, S. *J. Org. Chem.* **2008**, *73*, 738–740.
(16) Ford, W. E. *J. Photochem.* **1986**, *34*, 43–54.
(17) Feiler, L.; Langhals, H.; Polborn, K. *Liebigs Ann.* **1995**, 1229–1244.
(18) van der Boom, T.; Hayes, R. T.; Zhao, Y. Y.; Bushard, P. J.; Weiss, E. A.; Wasielewski, M. R. *J. Am. Chem. Soc.* **2002**, *124*, 9582–9590.
(19) Holman, M. W.; Liu, R.; Adams, D. M. *J. Am. Chem. Soc.* **2003**, *125*, 12649–12654.
(20) Ahrens, M. J.; Sinks, L. E.; Rybtchinski, B.; Liu, W. H.; Jones, B. A.; Giaimo, J. M.; Gusev, A. V.; Goshe, A. J.; Tiede, D. M.; Wasielewski, M. R. *J. Am. Chem. Soc.* **2004**, *126*, 8284–8294.
(21) Jones, B. A.; Ahrens, M. J.; Yoon, M. H.; Facchetti, A.; Marks, T. J.; Wasielewski, M. R. *Angew. Chem., Int. Ed.* **2004**, *43*, 6363–6366.
(22) Rybtchinski, B.; Sinks, L. E.; Wasielewski, M. R. *J. Phys. Chem. A* **2004**, *108*, 7497–7505.
(23) Rybtchinski, B.; Sinks, L. E.; Wasielewski, M. R. *J. Am. Chem. Soc.* **2004**, *126*, 12268–12269.
(24) Sinks, L. E.; Rybtchinski, B.; Iimura, M.; Jones, B. A.; Goshe, A. J.; Zuo, X.; Tiede, D. M.; Li, X.; Wasielewski, M. R. *Chem. Mater.* **2005**, *17*, 6295–6303.
(25) Sinks, L.; Fuller, M. J.; Liu, W.; Ahrens, M. J.; Wasielewski, M. R. *Chem. Phys.* **2005**, *319*, 226–234.
(26) Tauber, M. J.; Kelley, R. F.; Giaimo, J. M.; Rybtchinski, B.; Wasielewski, M. R. *J. Am. Chem. Soc.* **2006**, *128*, 1782–1783.
(27) Su, W.; Zhang, Y.; Zhao, C.; Li, X.; Jiang, J. *ChemPhysChem* **2007**, *8*, 1857–1862.
(28) Jones, B. A.; Facchetti, A.; Marks, T. J.; Wasielewski, M. R. *Chem. Mater.* **2007**, *19*, 2703–2705.
(29) Ahrens, M. J.; Kelley, R. F.; Dance, Z. E. X.; Wasielewski, M. R. *Phys. Chem. Chem. Phys.* **2007**, *9*, 1469–1478.
(30) Bullock, J. E.; Kelley, R. F.; Wasielewski, M. R. *PMSE Prepr.* **2007**, *96*, 805–806.
(31) Chaignon, F.; Falkenstrom, M.; Karlsson, S.; Blart, E.; Odobel, F.; Hammarstrom, L. *Chem. Commun.* **2007**, 64–66.
(32) Hrdlovic, P.; Chmela, S.; Danko, M. *J. Photochem. Photobiol., A* **1998**, *112*, 197–203.
(33) Schweitzer, G.; Gronheid, R.; Jordens, S.; Lor, M.; Belder, G. D.; Weil, T.; Reuther, E.; Muellen, K.; Schyver, F. C. D. *J. Phys. Chem. A* **2003**, *107*, 3199–3207.
(34) Holtrup, F. O.; Muller, G. R. J.; Quante, H.; De Feyter, S.; De Schryver, F. C.; Muellen, K. *Chem.−Eur. J.* **1997**, *3*, 219–225.
(35) Dance, Z. E. X.; Mi, Q.; McCamant, D. W.; Ahrens, M. J.; Ratner, M. A.; Wasielewski, M. R. *J. Phys. Chem. B* **2006**, *110*, 25163–25173.
(36) Hayes, R. T.; Walsh, C. J.; Wasielewski, M. R. *J. Phys. Chem. A* **2004**, *108*, 3253–3260.
(37) Li, X. Y.; Sinks, L. E.; Rybtchinski, B.; Wasielewski, M. R. *J. Am. Chem. Soc.* **2004**, *126*, 10810–10811.
(38) Fischer, M. K. R.; Kaiser, T. E.; Wuerthner, F.; Baeuerle, P. *J. Mater. Chem.* **2009**, *19*, 1129–1141.
(39) Chen, Z.; Baumeister, U.; Tschierske, C.; Wuerthner, F. *Chem.−Eur. J.* **2007**, *13*, 450–465.
(40) Baram, J.; Shirman, E.; Ben-Shitrit, N.; Ustinov, A.; Weissman, H.; Pinkas, I.; Wolf, S. G.; Rybtchinski, B. *J. Am. Chem. Soc.* **2008**, *130*, 14966–14967.
(41) Weissman, H.; Shirman, E.; Ben-Moshe, T.; Cohen, R.; Leitus, G.; Shimon, L. J. W.; Rybtchinski, B. *Inorg. Chem.* **2007**, *46*, 4790–4792.
(42) Sisson, A. L.; Sakai, N.; Banerji, N.; Fuerstenberg, A.; Vauthey, E.; Matile, S. *Angew. Chem., Int. Ed.* **2008**, *47*, 3727–3729.
(43) Dance, Z. E. X.; Mickley, S. M.; Wilson, T. M.; Ricks, A. B.; Scott, A. M.; Ratner, M. A.; Wasielewski, M. R. *J. Phys. Chem. A* **2008**, *112*, 4194–4201.
(44) Rajasingh, P.; Cohen, R.; Shirman, E.; Shimon, L. J. W.; Rybtchinski, B. *J. Org. Chem.* **2007**, *72*, 5973–5979.
(45) Golubkov, G.; Weissman, H.; Shirman, E.; Wolf, S. G.; Pinkas, I.; Rybtchinski, B. *Angew. Chem., Int. Ed.* **2009**, *48*, 926–930.
(46) Huang, J.; Wu, Y.; Fu, H.; Zhan, X.; Yao, J.; Barlow, S.; Marder, S. R. *J. Phys. Chem. A* **2009**, *113*, 5039–5046.
(47) Ahrens, M. J.; Tauber, M. J.; Wasielewski, M. R. *J. Org. Chem.* **2006**, *71*, 2107–2114.
(48) Fuller, M. J.; Sinks, L. E.; Rybtchinski, B.; Giaimo, J. M.; Li, X.; Wasielewski, M. R. *J. Phys. Chem. A* **2005**, *109*, 970–975.
(49) Rohr, U.; Schilichting, P.; Bohm, A.; Gross, M.; Meerholz, K.; Brauchle, C.; Muellen, K. *Angew. Chem., Int. Ed.* **1998**, *37*, 1434–1437.
(50) Miller, M. A.; Lammi, R. K.; Prathapan, S.; Holten, D.; Lindsey, J. S. *J. Org. Chem.* **2000**, *65*, 6634–6649.
(51) Rohr, U.; Kohl, C.; Muellen, K.; van de Craats, A.; Warman, J. *J. Mater. Chem.* **2001**, *11*, 1789–1799.
(52) Zhao, C.; Zhang, Y.; Li, R.; Li, X.; Jiang, J. *J. Org. Chem.* **2007**, *72*, 2402–2410.
(53) Nakazono, S.; Imazaki, Y.; Yoo, H.; Yang, J.; Sasamori, T.; Tokitoh, N.; Cedric, T.; Kageyama, H.; Kim, D.; Shinokubo, H.; Osuka, A. *Chem.−Eur. J.* **2009**, *15*, 7530–7533, S7530/7531−S7530/7525.
(54) Murai, S.; Kakiuchi, F.; Sekine, S.; Tanaka, Y.; Kamatani, A.; Sonoda, M.; Chatani, N. *Nature (London, U.K.)* **1993**, *366*, 529–531.
(55) Murai, S.; Kakiuchi, F.; Sekine, S.; Tanaka, Y.; Kamatani, A.; Sonoda, M.; Chatani, N. *Pure Appl. Chem.* **1994**, *66*, 1527–1534.
(56) Kakiuchi, F.; Sekine, S.; Tanaka, Y.; Kamatani, A.; Sonoda, M.; Chatani, N.; Murai, S. *Bull. Chem. Soc. Jpn.* **1995**, *68*, 62–83.

(57) Sonoda, M.; Kakiuchi, F.; Chatani, N.; Murai, S. *J. Organomet. Chem.* **1995**, *504*, 151–152.

(58) Sonoda, M.; Kakiuchi, F.; Kamatani, A.; Chatani, N.; Murai, S. *Chem. Lett.* **1996**, 109–110.

(59) Kakiuchi, F.; Sato, T.; Tsujimoto, T.; Yamauchi, M.; Chatani, N.; Murai, S. *Chem. Lett.* **1998**, 1053–1054.

(60) Kakiuchi, F.; Sato, T.; Igi, K.; Chatani, N.; Murai, S. *Chem. Lett.* **2001**, 386–387.

(61) Kakiuchi, F.; Murai, S. *Acc. Chem. Res.* **2002**, *35*, 826–834.

(62) Guo, H.; Tapsak, M. A.; Weber, W. P. *Polym. Bull. (Berlin)* **1994**, *33*, 417–423.

(63) Guo, H.; Weber, W. P. *Polym. Bull. (Berlin)* **1994**, *32*, 525–528.

(64) Gupta, S. K.; Weber, W. P. *Macromolecules* **2002**, *35*, 3369–3373.

(65) Murai, S.; Chatani, N.; Kakiuchi, F. *Pure Appl. Chem.* **1997**, *69*, 589–594.

(66) Kakiuchi, F.; Murai, S. *Org. Synth.* **2003**, *80*, 104–110.

(67) Connelly, N. G.; Geiger, W. E. *Chem. Rev.* **1996**, *96*, 877–910.

(68) Kelley, R. F.; Shin, W. S.; Rybtchinski, B.; Sinks, L. E.; Wasielewski, M. R. *J. Am. Chem. Soc.* **2007**, *129*, 3173–3181.

(69) Shao, Y.; Molnar, L. F.; Jung, Y.; Kussmann, J.; Ochsenfeld, C.; Brown, S. T.; Gilbert, A. T. B.; Slipchenko, L. V.; Levchenko, S. V.; O'Neill, D. P.; DiStasio, R. A.; Lochan, R. C.; Wang, T.; Beran, G. J. O.; Besley, N. A.; Herbert, J. M.; Lin, C. Y.; Van Voorhis, T.; Chien, S. H.; Sodt, A.; Steele, R. P.; Rassolov, V. A.; Maslen, P. E.; Korambath, P. P.; Adamson, R. D.; Austin, B.; Baker, J.; Byrd, E. F. C.; Dachsel, H.; Doerksen, R. J.; Dreuw, A.; Dunietz, B. D.; Dutoi, A. D.; Furlani, T. R.; Gwaltney, S. R.; Heyden, A.; Hirata, S.; Hsu, C. P.; Kedziora, G.; Khalliulin, R. Z.; Klunzinger, P.; Lee, A. M.; Lee, M. S.; Liang, W.; Lotan, I.; Nair, N.; Peters, B.; Proynov, E. I.; Pieniazek, P. A.; Rhee, Y. M.; Ritchie, J.; Rosta, E.; Sherrill, C. D.; Simmonett, A. C.; Subotnik, J. E.; Woodcock, H. L.; Zhang, W.; Bell, A. T.; Chakraborty, A. K.; Chipman, D. M.; Keil, F. J.; Warshel, A.; Hehre, W. J.; Schaefer, H. F.; Kong, J.; Krylov, A. I.; Gill, P. M. W.; Head-Gordon, M. *Phys. Chem. Chem. Phys.* **2006**, *8*, 3172–3191.

(70) Improta, R.; Barone, V. *Chem. Rev.* **2004**, *104*, 1231–1253.

(71) Frisch, M. J.; Trucks, G. W.; Schlegel, H. B.; Scuseria, G. E.; Robb, M. A.; Cheeseman, J. R.; Zakrzewski, V. G.; J. A. Montgomery, J.; Stratmann, R. E.; Burant, J. C.; Dapprich, S.; Millam, J. M.; Daniels, A. D.; Kudin, K. N.; Strain, M. C.; Farkas, O.; Tomasi, J.; Barone, V.; Cossi, M.; Cammi, R.; Mennucci, B.; Pomelli, C.; Adamo, C.; Clifford, S.; Ochterski, J.; Petersson, G. A.; Ayala, P. Y.; Cui, Q.; Morokuma, K.; Malick, D. K.; Rabuck, A. D.; Raghavachari, K.; Foresman, J. B.; Cioslowski, J.; Ortiz, J. V.; Baboul, A. G.; Stefanov, B. B.; Liu, G.; Liashenko, A.; Piskorz, P.; Komaromi, I.; Gomperts, R.; Martin, R. L.; Fox, D. J.; Keith, T.; Al-Laham, M. A.; Peng, C. Y.; Nanayakkara, A.; Gonzalez, C.; Challacombe, M.; Gill, P. M. W.; Johnson, B.; Chen, W.; Wong, M. W.; Andres, J. L.; Gonzalez, C.; Head-Gordon, M.; Replogle, E. S.; Pople, J. A. *Gaussian 98W, Revision A.7;* Gaussian, Inc.: Pittsburgh, PA, 1998.

(72) Kakiuchi, F.; Chatani, N. *Top. Organomet. Chem.* **2004**, *11*, 45–79.

(73) Licchelli, M.; Linati, L.; Biroli, A. O.; Perani, E.; Poggi, A.; Sacchi, D. *Chem—Eur. J.* **2002**, *8*, 5161–5169.

(74) Giaimo, J. M.; Lockard, J. V.; Sinks, L. E.; Scott, A. M.; Wilson, T. M.; Wasielewski, M. R. *J. Phys. Chem. A* **2008**, *112*, 2322–2330.

(75) Ganesan, P.; Baggerman, J.; Zhang, H.; Sudhoelter, E. J. R.; Zuilhof, H. *J. Phys. Chem. A* **2007**, *111*, 6151–6156.

(76) Marcus, R. A. *J. Chem. Phys.* **1956**, *24*, 966–978.

(77) Kurreck, H.; Kirste, B.; Lubitz, W. *Electron Nuclear Double Resonance Spectroscopy of Radicals in Solution*; VCH: Weinheim, Germany, 1988.

(78) Wilson, T. M.; Tauber, M. J.; Wasielewski, M. R. *J. Am. Chem. Soc.* **2009**, *131*, 8952–8957.

(79) Duling, D. R. *J. Magn. Reson. B* **1994**, *104*, 105–110.

JP908679C